Electronic Supplementary Material (ESI) for Analyst.

Determination of the Transfer Function of an Atmospheric Pressure Drift Tube Ion Mobility Spectrometer for Nanoparticle Measurements

David T. Buckley & Christopher J. Hogan Jr.*

Department of Mechanical Engineering, University of Minnesota, Minneapolis, MN, USA

SUPPLEMENTAL INFORMATION

***To whom correspondence should be addressed: hogan108@ umn.edu, Tel: 1-612-626-8312, Fax: 1-612-625-6069.**

Information Available

- Theoretical description of the DMA transfer function
- Comparison of $y|_{t^*,K^*}$ and $\theta_D|_{K^*}$
- Parameterization of Q_I as skewed Gaussian functions
- Theoretical description of θ_I, DT-IMS transfer function
- The CPC response time distribution function

Theoretical Description of the DMA Transfer Function

Knowledge of the DMA transfer function and the transmission of particles through system tubing is necessary in particular for application of equation (2) and generally for use of the Twomey-Markowski algorithm for transfer function inversion. For nanometer-scale particles, diffusion is the main contributor to transfer function broadening in the DMA. The transfer function provided by Stolzenburg and McMurry,[1] which accounts for particle diffusion, is given as:

$$\theta_D|_{K^*} = \frac{\sigma}{\sqrt{2}\beta}\left[erf\left(\frac{\widetilde{K}-(1+\beta)}{\sqrt{2}\sigma}\right) + erf\left(\frac{\widetilde{K}-(1-\beta)}{\sqrt{2}\sigma}\right) - 2erf\left(\frac{\widetilde{K}-1}{\sqrt{2}\sigma}\right)\right] \quad \text{(S1)}$$

where σ represents the non-dimensional standard deviation of the mobility distribution exiting the DMA, β is the ratio of the aerosol to sheath flowrate, and $\widetilde{K}$ is the particle mobility normalized by the mobility at which particles are maximally transmitted through the DMA, K^*. *erf* signifies that the error function is applied to the argument following in parentheses. $\widetilde{K}$ is defined by:

$$\widetilde{K} = \frac{K}{K^*} \quad \text{(S2a)}$$

K^* is calculated by:

$$K^* = \frac{Q_{sh}\ln(\frac{R_2}{R_1})}{2\pi LV} \quad \text{(S2b)}$$

where Q_{sh} is the volumetric sheath flowrate in the DMA, R_2 and R_1 are the respective outer and inner radii of the DMA, L is the DMA length, and V is the voltage applied across the DMA electrodes.

σ is the standard deviation of the mobility distribution exiting the DMA, defined by:

$$\sigma^2 = G_{DMA} * \widetilde{D} \quad \text{(S3)}$$

G_{DMA} is a non-dimensional geometry factor and $\widetilde{D}$ is:

$$\widetilde{D} = \frac{2\pi LD}{Q_{sh}} = \frac{2\pi Lk_BTK}{Q_{sh}ze} \quad \text{(S4)}$$

where D is the particle diffusion coefficient, k_B is the Boltzmann constant, T is particle temperature (assumed to be that of the surrounding gas), and ze is the total charge on the particle. Particles are typically singly charged (z = 1) in this study.

Because diffusion is the main contributor to transfer function broadening in any DMA, overall resolving power can be improved by decreasing particle residence time in the DMA. This is accomplished by increasing both the sheath flow and the potential applied across the DMA electrodes. Unfortunately, the transition to turbulence at high sheath flows perturbs particle streamlines, significantly affecting instrument resolution and reducing the predictability of mobility-dependent particle transmission. Transition to turbulence limits the TSI nano-DMA sheath flow and resolution to maxima of ~15 l min^{-1} and ~10 (with higher sheath flowrates often leading to non-idealized behavior), respectively. This low sheath flowrate is simple to control and measure, and because all other relevant parameters are well-characterized, the use of equation (S1) to describe particle transmission through the nano-DMA is straightforward.

Comparison of $y|_{t^*,K^*}$ and $\theta_D|_{K^*}$

Figure S1a displays selected measured values, $y|_{t^*,K^*}$, for various t^* values (red). Also plotted are the nano-DMA transfer functions for the K^* corresponding to the peak mobility of the measured values. The nano-DMA transfer functions have been scaled (arbitrarily, as they are dimensionless functions) to have the same maximum value as the $y|_{t^*,K^*}$, to better facilitate comparison. For a high resolving power DT-IMS-CPC, $Q_I|_{t^*}$, is narrowly distributed, and $y|_{t^*,K^*}$ would be distributed only by $\theta_D|_{K^*}$, the nano-DMA transfer function. Therefore, the scaled nano-DMA transfer functions shown in figure S1 represent the measured $y|_{t^*,K^*}$ for a perfect DT-IMS-CPC. In reality, $Q_I|_{t^*}$ has a finite width, and the difference in shape between the scaled nano-DMA transfer function and the $y|_{t^*,K^*}$ represents the true DT-IMS-CPC transfer function, $Q_I|_{t^*}$. These differences are quantified by employing the Twomey-Markowski algorithm.

To further illustrate that the DMA and DT-IMS need to be similar in resolving power, figure S1b focuses on the measured $y|_{t^*,K^*}$ values (red circles) for t^* = 6 s, displaying again the scaled nano-DMA transfer function (black line) along with several simulated $y|_{t^*,K^*,sim}$ values (triangles). $y|_{t^*,K^*,sim}$ were calculated through computation of the integral on the RHS of equation (4a) by assuming the skew Gaussian form of $Q_I|_{t^*}$ (determined in the main text) and varying the scale factor of $Q_I|_{t^*}$. This results in variable transfer function width, or resolution, with the adjusted resulting resolving powers noted in the figure caption. The pink triangles in figure S1b demonstrate that for a DT-IMS-CPC with high resolution (>70), the $y|_{t^*,K^*,sim}$ collapse to the scaled nano-DMA transfer function. As simulated instrument resolving power decreases, $y|_{t^*,K^*,sim}$ becomes increasingly broad relative to the DMA transfer function.

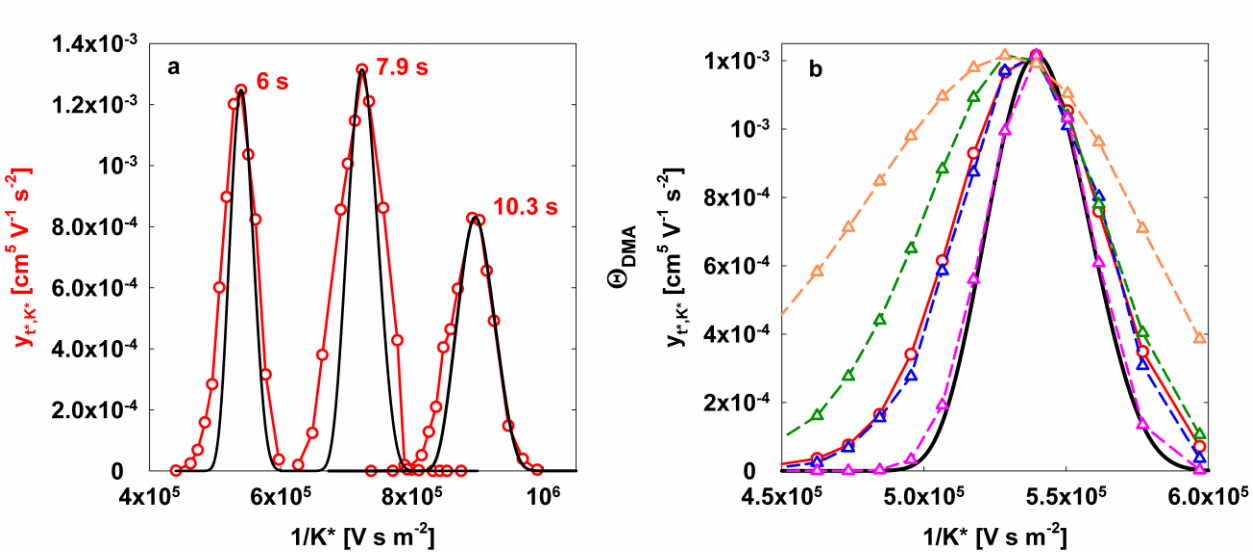

Figure S1. (a) Selected measured $y|_{t^*,K^*}$ for various t* values (red) along with the nano-DMA transfer function for the K^* corresponding to the peak signal of the measured values are plotted. The nano-DMA transfer functions have been scaled to have the same peak value as the measured values for the sake of comparison. **(b)** $y|_{t^*,K^*}$ for $t^* = 6\,s$ (red circles) and the nano-DMA transfer function (black line - normalized to the measured values) corresponding the K^* at which the measured values are peaked along with several simulated $y|_{t^*,K^*,sim}$ values (triangles) calculated for varying DT-IMS-CPC transfer function widths. The simulated $y|_{t^*,K^*}$ values were calculated by varying the DT-IMS-CPC transfer function according to its resolution; pink corresponds to a high resolution system (R = 73), blue to the current DT-IMS-CPC (R = 13.3), green to a system with similar resolution to that of the nano-DMA (R = 8.8), and orange to a low resolving power system (R = 5). The simulated $y|_{t^*,K^*}$ values have been normalized in magnitude to the same peak value for the sake of comparison.

Parameterization of Q_I as Skewed Gaussian Functions

The skewed Gaussian distribution can be described simply as a Gaussian distribution multiplied by its cumulative distribution function. The functional form used in this work is a typical skewed Gaussian with an additional multiplicative scaling factor:

$$Q_{I,P}\big|_{m,s,A,\propto} = 2 * A * \Phi|_{m,s,\alpha} * \varphi|_{m,s} \quad \text{(S5)}$$

where $\varphi|_{m,s}$ is a standard Gaussian probability density function which is distributed in inverse mobility and defined by its mean, m, and standard deviation, s: $\varphi|_{m,s} = \frac{1}{\sqrt{2s^2\pi}} e^{-\frac{(1/K-m)^2}{2s^2}}$. $\Phi|_{m,s,\propto}$ is the cumulative distribution function of the skewed Gaussian with an additional factor, α, which affects the skew of the final distribution. The parameter A is used as an amplitude scaling factor.

As described in the main text, each inverted $Q_I|_{t^*}$ was fitted parametrically to equation S5 using MATLAB's non-linear fitting procedure, resulting in data relating the skew Gaussian parameters (α, m, s, and A) to t^*. These skewed Gaussian parameters are shown as functions of t^* with their best fit curves in figures S2a-f. Separate fits for both s and A were performed before and after $t^* = 9.5\,s$ because the relationship between the parameters and t* changed after $t^* = 9.5\,s$. The average value for α at t^* < 9.5 s was used for all parameterizations and fits. Error parameters are shown in figures (S2g,h). The low R^2 for t* > 11.5 s is most likely due to the use of a constant α for all t*.

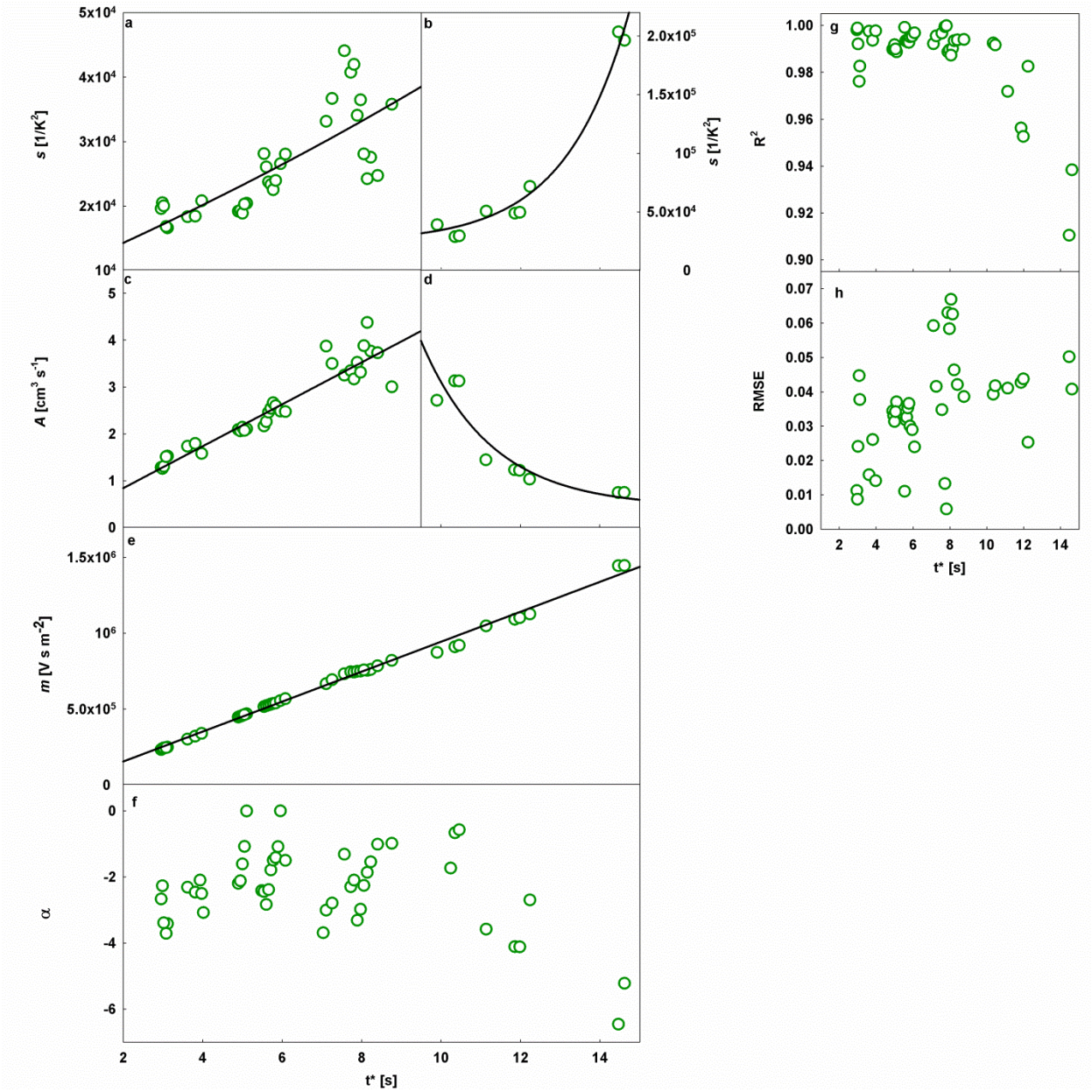

Figure S2a-f. Parameters which resulted from fitting the modified skew Gaussian to the inverted Q_I data for all t^* values. **(S2g, h)** Fit error evaluation. The parameters plotted are location – m (**a**), scale - s (**b, c**), amplitude – A (**d, e**), and shape - α (**f**). The errors represented are the R-squared value of the fit (**g**) and the Root-mean-squared error of the fit (**h**).

DT-IMS Transfer Function, θ_I

The transfer function of an aspirating, fluid mechanically gated DT-IMS was derived previously[2] through modification of the original derivation by Revercomb and Mason[3] by accounting for both the effect of the counter flow and the finite width of the initial ion pulse. The DT-IMS transfer function is defined as a Gaussian function distributed in time with width defined by both diffusional broadening and the initial width of the ion pulse:

$$\theta_I = \sqrt{\frac{2\ln(2)}{\pi}}\frac{1}{\Delta t_d} \times \exp\left(-4\ln(2)\left[\frac{t_d - t_{ave}}{\Delta t_d}\right]^2\right) \quad \text{(S6)}$$

where t_d, the drift time, denotes the time necessary for a particle to reach the CPC inlet, t_{ave} represents the average drift time for particles of mobility *K*, and Δt_d is the FWHM of the distribution. t_{ave} and Δt_d are defined theoretically:

$$t_{ave} = \frac{L}{v_d} = \frac{L * L_E}{KV} \quad \text{(S7)}$$

where L is the DT-IMS length, and v_d, the drift velocity, is calculated simply through the definition of electrical mobility: $v_d = KE = \frac{KV}{L_E}$. L_E is the distance between the first and last electrodes, and *V* is the applied voltage to the DT-IMS. Δt_d is calculated by combining the effect of diffusional broadening and the initial width (transformed to its effect in drift time) of the sample volume:

$$(\Delta t_d)^2 = (\Delta t_0)^2 + \frac{(k_B T)}{ze(V - \frac{u_c L}{K})} 16\ln(2) {t_{ave}}^2 \quad \text{(S8)}$$

where Δt_0 represents the half width of the sample volume converted to time, again via the particle drift velocity: $\Delta t_0 = \frac{\Delta x}{v_d}$, where Δx is the half width in distance of the sample volume, estimated to be 0.8 cm in Oberreit et al.[2] k_B is the Boltzmann constant, *T* is temperature of the surrounding gas, *z* is the integer charge on the particle, *e* is the electron charge, *V* is the applied

voltage to the DT-IMS, and u_c is the centerline velocity of the counterflow (calculated by dividing the volume flowrate by the cross-sectional area of the DT-IMS).

CPC Response Time Distribution, Φ_C

The response time distribution, Φ_C, of the WCPC (Model 3786, TSI, inc., Shoreview, MN) was measured previously[2] and is displayed again in figure S3 as a function of time in the CPC, t_C. In order to perform the calculations described in the correction factor function determination, the response time distribution function data were represented continuously in time by interpolating using MATLAB's spline interpolation algorithm.

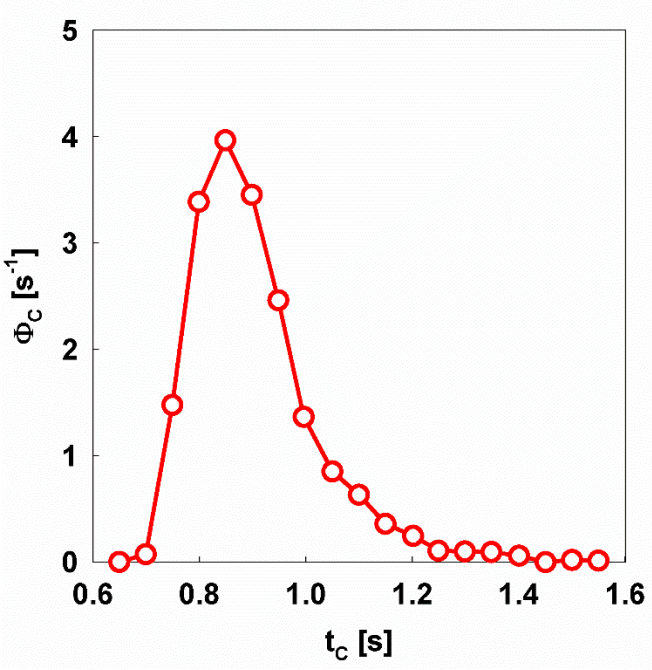

Figure S3: Response time distribution function of the TSI WCPC Model 3786, reported in Oberreit et al (2014)[2]. The distribution peak value is t_C = 0.846 s.

REFERENCES

[1]M. R. Stolzenburg and P. H. McMurry, Aerosol Science and Technology **42,** (2008) 421-432.
[2]D. R. Oberreit, P. H. McMurry and C. J. Hogan, Aerosol Science & Technology **48,** (2014) 108-118.
[3]H. E. Revercomb and E. A. Mason, Analytical Chemistry **47,** (1975) 970-983.